

A New Application of UV–Ozone Treatment in the Preparation of Substrate-Supported, Mesoporous Thin Films

Theotis Clark, Jr.,^{†,‡} Julia D. Ruiz,^{§,‡} Hongyou Fan,^{||,⊥} C. Jeffrey Brinker,^{*,||,⊥}
Basil I. Swanson,[‡] and Atul N. Parikh^{*,‡}

Bioscience Division, Los Alamos National Laboratory, Los Alamos, New Mexico 87545,
University of New Mexico/NSF Center for Micro-Engineered Materials, The Advanced
Materials Laboratory, 1001 University Boulevard SE, Albuquerque, New Mexico 87106, and
Department 1831, Sandia National Laboratories, Albuquerque, New Mexico 87131

Received June 6, 2000. Revised Manuscript Received August 25, 2000

A nominally room temperature photochemical method, simply employing ultraviolet light (187–254 nm) generated ozone environment, is shown to provide an efficient alternative for the removal of surfactant templates for a routine production of mesoporous silica thin films at low temperatures. The treatment concomitantly strengthens the silicate phase by fostering the condensation of unreacted silanols leading to mesoporous thin films with well-defined mesoscopic morphologies. The surfactant/silicate thin film mesophases were prepared onto a polycrystalline Au surface by dip-coating or spin-casting methods using sub-critical micelle concentration (cmc) nonionic ethylene oxide surfactant in an oligomeric silica sol mixture. The structures and compositions of the thin film mesophases before and after exposure to UV/ozone were determined using a combination of reflection–absorption Fourier transform infrared spectroscopy, transmission electron microscopy, and thin film X-ray diffraction measurements. The pore characteristics of the UV/ozone-treated films were determined using nitrogen adsorption/desorption isotherm measurements. Results presented here clearly establish that the UV/ozone processing leads to complete removal of the surfactant template; strengthens the inorganic skeleton by fostering silica condensation; and renders the mesophase thin film surfaces highly hydrophilic. Two of the most attractive features of the method developed here, namely its usefulness in applications for temperature intolerant substrates (e.g., thin metal films) and in spatially selective removal of the surfactant templates to create patterns of mesoporous thin films, are also illustrated. Finally, the mechanistic implications of these observations are also discussed.

Introduction

The cooperative self-assembly of amphiphiles and oligomeric silica precursors on solid surfaces can produce a wide range of inorganic mesoporous thin film materials with controllable morphologies and surface characteristics.^{1–7} These films hold considerable promise in a host of technologies including, shape- and size-

selective surface catalysis,⁸ microelectrochemistry,⁹ low dielectric constant thin films, and biological and chemical sensing and detection,¹⁰ as well as in a host of fundamental studies involving laterally confined surface chemical and biochemical reactions. But many of these applications require selective removal of the organic phase from the precursor organic–inorganic mesostructured thin film, currently accomplished using high-temperature thermal-chemical calcination processes. The latter processes, owing to their aggressive thermal and/or chemical environments, often damage important physical–chemical characteristics of the underlying substrate surfaces, thus limiting the usefulness of the

[†] University of California President's Postdoctoral Scholar.

[‡] Los Alamos National Laboratory.

[§] Participant, Underrepresented Minority Student Program, Los Alamos National Laboratory.

^{||} The Advanced Materials Laboratory.

[⊥] Sandia National Laboratories.

* Corresponding authors (E-mail: parikh@lanl.gov; cjbrink@sandia.gov).

(1) Ogawa, M. *J. Am. Chem. Soc.* **1994**, *116*, 7941–7942; *Chem. Commun.* **1996**, *10*, 1149–1150.

(2) Aksay, I. A.; et al. *Science* **1996**, *273*, 892–898.

(3) (a) Yang, H.; Kuperman, A.; Coombs, N.; Mamicheafara, S.; Ozin, G. A. *Nature* **1996**, *379*, 703–705. (b) Yang, H.; Coombs, N.; Sokolov, I.; Ozin, G. A. *Nature* **1996**, *381*, 589–592.

(4) (a) Brinker, C. J. *Curr. Opin. Coll. Interface Sci.* **1998**, *3*, 166–173. (b) Sellinger, A.; Weiss, P. M.; Nguyen, A.; Lu, Y.-F.; Assink, R. A.; Gong, W. L.; Brinker, C. J. *Nature* **1998**, *394*, 256–260. (c) Lu, Y. F.; et al. *Nature* **1997**, *389*, 364–368.

(5) Tolbert, S. H.; Schaffer, T. E.; Feng, J. L.; Hansma, P. K.; Stucky, G. D. *Chem. Mater.* **1997**, *9*, 1962–1967.

(6) Miyata, H.; Kuroda, K. *J. Am. Chem. Soc.* **1999**, *121*, 7618–7624; *Chem. Mater.* **1999**, *11*, 1609–1614.

(7) (a) Zhao, D. Y.; Yang, P. D.; Margolese, D. I.; Chmelka, B. F.; Stucky, G. D. *Chem. Commun.* **1998**, *22*, 2499–2500. (b) Zhao, D. Y.; Yang, P. D.; Melosh, N.; Feng, J.; Chmelka, B. F.; Stucky, G. D. *Adv. Mater.* **1998**, *10*, 1380.

(8) See, for example: (a) Corma, A. *Chem. Rev.* **1997**, *97*, 2373–2419. (b) Vartuli, J. C.; Shih, S. S.; Kresge, C. T.; Beck, J. S. *Stud. Surf. Sci. Catal.* **1998**, *117*, 13–21.

(9) Attard, G. S.; Bartlett, P. N.; Coleman, N. R. B.; Elliot, J. M.; Owen, J. R.; Wang, J. H. *Science* **1997**, *279*, 838–840.

(10) See, for example: GimonKinsel, M. E.; Balkus, K. J. *Stud. Surf. Sci. Catal.* **1998**, *117*, 111–118.

approach in applications wherein the substrate surface characteristics are highly temperature-sensitive, e.g., thin metal films.

In this regard, it appears that room-temperature exposure to ozone will provide a nonthermal alternative for the removal of the organic template phase from thin film silica mesophases. The use of ozone in removing organic "contaminants" has been well recognized and widely implemented, for example, in water treatment¹¹ and in semiconductor technologies for cleaning semiconductor substrate surfaces.¹² However, its use in removing template microphases from organically templated inorganic materials is rare. To the best of our knowledge, only one such effort has been reported.¹³ In a recent study by Keene and co-workers,¹³ it was shown that an extended exposure (~24 h) to ozone (produced in-situ photochemically as well as gaseous ozone) can be used to remove the template surfactants from bulk three-dimensional (3D) MCM-41 type materials. Despite its obvious potential, the use of the method for removal of template from two-dimensional (2D) thin film mesophases, selective area template removal or pattern formation, and for mesophase films on temperature-intolerant substrates is not yet explored. Furthermore, the mechanism by which ozone treatment leads to mesoporous materials remains poorly understood. That UV/ozone environment removes the surfactant template is appreciated in the study by Keene and co-workers;¹³ the roles of UV light (in addition to producing ozone) and the effects of the UV/ozone exposure on the inorganic phase are not understood. These issues are addressed in this paper.

First, we confirm that the room-temperature photochemical treatment involving in-situ production of ozone provides a useful alternative for efficient and complete removal of the surfactant template from 2D thin film mesophases on a wide variety of substrates including temperature-intolerant thin metal films. We show for the first time that the method, in addition to removing the organic template phase, leads to a substantial reconstruction of the silicate skeleton via increased silica condensation.¹⁴ Finally, we show that the method offers an elegant control for rapid and laterally selective template removal (e.g., patterned mesostructured/mesoporous films) over the conventional thermal-chemical processes. Mechanistic implications of the success in patterning the surfactant silicate mesophases using UV/ozone treatment are also discussed.

Our nominally room-temperature photochemical method involves simply the exposure of the as-formed, substrate-supported surfactant-silicate thin film mesophases to ultraviolet (UV) light ($\lambda = 184\text{--}257\text{ nm}$) produced by a low-pressure Hg discharge grid-lamp in quartz envelope, maintained in a closed chamber under laboratory ambient conditions. It is now well established

that the mechanism by which UV/ozone destroys the organics involves a complex set of photosensitized oxidation processes.^{15,16} The simplest description of the overall process involves three overlapping photoinduced chemical reactions. First, UV light with a wavelength below 245.4 nm (optimally at $\lambda = 184\text{ nm}$) facilitates the dissociation of oxygen (from the ambient) to produce ozone and atomic oxygen. Simultaneously, the 253.7 nm line emitted by the same lamp excites and/or dissociates the organic matrix in the thin film mesophases, thereby producing activated species, such as ions, free radicals, and excited molecules. Finally, the activated organic species are readily attacked by atomic oxygen and ozone synergistically to form simpler volatile molecules, such as CO_2 , H_2O , N_2 , etc., which escape the film interior and/or are simply washed off in subsequent solvent and water rinses.

The required exposure time, 60–120 min for the complete removal of the surfactant precursor, was found to depend on the cleanliness of the UV generating lamp, distance of the sample from the lamp, and the thickness of the thin film mesophase. Although the UV/ozone treatment is employed at room temperature, local temperature at the substrates during the process may increase to 40–50 °C. In contrast, the currently used thermal calcination process employs temperatures in excess of 400–500 °C and often requires several hours for the complete removal of the template.

Experimental Section

Amphiphile-templated organic-inorganic hybrid films were deposited onto evaporated gold substrates by adopting a previously published procedure.⁴ Briefly, the precursor solution was prepared by addition of a nonionic surfactant ($\text{C}_{16}\text{H}_{33}(\text{OCH}_2\text{CH}_2)_{10}\text{OH}$, technical name: Brij56, Aldrich) to an oligomeric silica sol solution at initial concentrations (C_0) ranging from 1.5 to 5.0 wt %, significantly below the critical micellar concentration (cmc). The silica sol in turn was prepared by refluxing a mixture of 56.9 g tetraethyl orthosilicate (TEOS, $\text{Si}(\text{OC}_2\text{H}_5)_4$), 48.1 g ethanol, 0.44 g water, and 0.51 mg 0.07 N hydrochloric acid (HCl) at 60 °C. During the addition of the surfactant, the water, ethanol, and hydrochloric acid concentrations were adjusted to yield the final reactant mixture in the following mole ratios: 1 TEOS/22 $\text{C}_2\text{H}_5\text{OH}$ /5 H_2O /0.004 HCl/0.054–0.18 surfactant. Films were deposited onto freshly oxidized single-crystal silicon (100) with native oxide overlayer (SiO_2/Si) and freshly evaporated 2000 Å Au metal films supported on freshly oxidized SiO_2/Si with a 50 nm Ti primer as an adhesion promoter. Both dip-coating and spin-coating procedures were used. Dip-coated samples were prepared by withdrawing the substrates from the precursor solution (see above) at ~4–38 cm/min. Spin-coated samples were derived by spinning the substrates at ~3000 rpm under ~1 mL of the precursor sol mixture for 120 s. The mesostructures of the substrate-supported thin films derived were verified using a combination of thin film X-ray diffraction (XRD), transmission electron microscopy (TEM), and Fourier transform infrared spectroscopy (FT-IR).

X-ray diffraction spectra were recorded on a Siemens D500 diffractometer using Ni-filtered $\text{CuK}\alpha$ radiation with $\lambda = 1.5406\text{ \AA}$ in θ - 2θ ($2\theta = 0.6\text{--}10^\circ$) scan mode using a step size of 0.02 and 0.5°/min. TEM measurements were performed on a JEOL 2010 with 200 kV accelerating voltage, equipped with a Gatan slow scan charge-coupled device (CCD) camera. The

(11) See, for example: Legrini, O.; Oliveros, E.; Braun, A. M. *Chem. Rev.* **1993**, *93*, 671–698 and references therein.

(12) See, for example: Tabe, M. *Appl. Phys. Lett.* **1984**, *45*, 1073–1075.

(13) (a) Keene, M. T. J.; Denoyel, R.; Llewellyn, P. L. *Chem. Commun.* **1998**, *20*, 2203–2204. (b) The abstract of this paper 13(a) incorrectly reports that the ozone treatment was carried out at 250 °C. The experiments presented were performed at room temperature.

(14) This conclusion is in disagreement with that reached for bulk MCM-41 type materials in the previous study by Keene and co-workers (ref 13) (see Results and Discussion).

(15) See, for example: (a) Vig, J. R. *J. Vac. Sci. Technol. A* **1985**, *3*, 1027–1033 and selected references therein.

(16) Zhang, Y.; Terrill, R. H.; Bohn, P. W. *Chem. Mater.* **1999**, *11*, 2191–2198.

sample was prepared by carefully scratching off the films on gold substrates using a pair of tweezers. To prepare the cross-sectional sample, a thin film was glued, cut, and polished until it was optically transparent (less than 1 mm) in the cross-sectional direction, then an ion-milling technique was used to further reduce the sample thickness until the sample was electron-transparent. FT-IR spectra were obtained in grazing incidence specular reflection mode at an 80° angle of incidence. Spectra were collected using an air-purged (CO_2 , H_2O free), Bruker Equinox Fourier Transform Infrared Spectrophotometer (Bio-Rad, Cambridge, MA). The incoming IR radiation was focused on the sample with an $\sim f/10$ optics and the reflected beam was detected using a narrow-band mercury–cadmium–tellurium (MCT) detector cooled with liquid nitrogen. A wire-grid polarizer was placed immediately before the sample and oriented to give p -polarization. All reported spectra were obtained by co-adding multiple scans collected at 2 cm^{-1} resolution. The interferograms were Fourier transformed with triangular apodization and with zero filling in order to increase the spectral point density to give $\sim \pm 0.5\text{ cm}^{-1}$ errors in point positions. Spectral intensities are reported in absorbance units of $-\log(R/R_0)$ where R and R_0 are the sample and reference reflectivities. Reference samples used were the freshly evaporated gold films immediately prior to the film deposition. A surface acoustic wave (SAW) technique was used to characterize N_2 desorption–adsorption isotherms of mesoporous thin film samples. The samples of thin film for SAW measurement were prepared directly onto ST-cut quartz SAW substrates. The SAW devices (97 MHz) on ST-quartz with Ti-primed Au transducers were custom-fabricated. In a typical acoustic wave device, an alternating voltage applied to an interdigital transducer on a piezoelectric substrate generates an alternating strain, which launches an acoustic wave. An Accelerated Surface Area and Porosimetry (ASAP) instrument was combined with the SAW device to control the relative pressure, while the SAW device was used to determine the frequency. Mass change was monitored ($\sim 80\text{ pg cm}^{-2}$ sensitivity) as a function of relative pressure, assuming that the SAW frequency is only perturbed by a mass loading variation. Surface area was estimated by using the Brunauer–Emmet–Teller (BET) equation. The pore size was calculated by modeling the pore as cylinders: the hydraulic radius $r = 2V/S$, where V is the pore volume and S is the surface area.

Results and Discussion

It was recently proposed that the preferential evaporation of ethanol from the wetting meniscus at the substrate surface drives the local surfactant concentration (C_s) to exceed its bulk cmc, thereby developing micellar microphases of the surfactants through local surface enrichment while maintaining the surfactant–silicate ratio nominally constant.^{2,4} This facilitates interfacial cooperative assembly of the surfactant mesophases¹⁷ and silica precursors¹⁸ to form continuous mesostructured films at the substrate surface. As discussed below, the organic–inorganic films prepared using ethylene-oxide surfactants were in the hexagonal phase and upon template removal were transformed into a thin film cubic mesoporous phase.

Central evidence establishing the selective and complete removal of the organic surfactant phase during the UV/ozone treatment was furnished by FT-IR measurements (Figure 1). The dashed traces in Figure 1(a) and (b) show the characteristic signature due to methylene ($-\text{CH}_2$) and methyl ($-\text{CH}_3$) C–H stretching vibrations¹⁹ from the surfactant microphases in the $2700\text{--}3100\text{ cm}^{-1}$

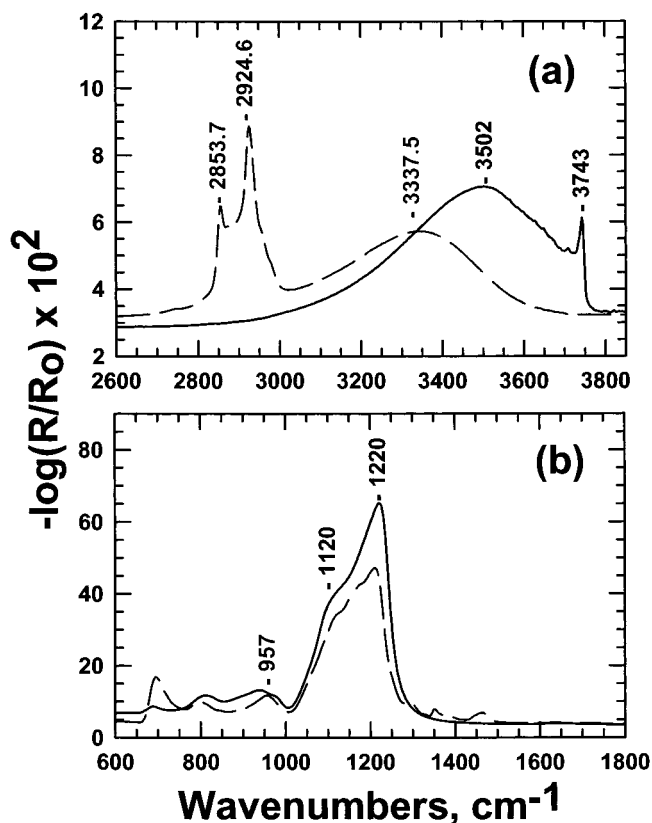


Figure 1. Grazing-incidence (80° incidence, p -polarized light) reflection–absorption spectra for brij56/TEOS films dip-coated on freshly evaporated Au films. The dashed trace shows the spectral features for the as-deposited film samples and the solid trace shows the spectral signature for the UV/ozone-treated samples.

region. In sharp contrast to the above, in the UV/ozone-treated samples these peaks are noticeably absent (vanishing below the noise level in our spectra), unambiguously confirming the near-complete removal (well below 1%) of the organic matrix from the initial films. Further details of the mesostructured films prior to the UV/ozone treatment can be deduced by a careful examination of the peak characteristics of the C–H stretching modes due to the absorptions by the surfactant chains. Specifically, the strong peak maxima at 2854.6 and 2924.6 cm^{-1} are assigned to $-\text{CH}_2$ -symmetric (d^+) and antisymmetric (d^-) stretching mode absorptions, whereas the overlapping contributions (reproducibly resolved in deconvoluted spectra) at 2873.4 and 2957.8 cm^{-1} are straightforwardly assigned to the $-\text{CH}_3$ symmetric (r^+) and antisymmetric (r^-) stretching mode absorptions. Because the peak positions for d^+ and d^- modes of alkyl chains are reported typically to be in the range $2846\text{--}2850$ and $2915\text{--}2918\text{ cm}^{-1}$ for all-trans extended chains²⁰ in crystalline matrixes and at ~ 2856 and $\sim 2928\text{ cm}^{-1}$ for disordered chains,²¹ in the molten or liquid state, the observed intermediate frequencies

(17) Manne, S.; Gaub, H. E. *Science* **1995**, *270*, 1480–1482.

(18) Brinker, C. J.; Scherer, G. W. *Sol-Gel Science: the Physics and Chemistry of Sol-Gel Processing*; Academic Press: New York, 1990.

(19) (a) Snyder, R. G.; Schachtschneider, J. H. *Spectrochim. Acta* **1963**, *19*, 85–116. (b) MacPhail, R. A.; Strauss, H. L.; Snyder, R. G.; Elliger, C. A. *J. Phys. Chem.* **1982**, *88*, 334–341. (c) Snyder, R. G.; Strauss, H. L.; Elliger, C. A. *J. Phys. Chem.* **1982**, *86*, 5145–5150.

(20) (a) Snyder, R. G.; Schachtschneider, J. H. *Spectrochim. Acta* **1963**, *19*, 85–116. (b) MacPhail, R. A.; Strauss, H. L.; Snyder, R. G.; Elliger, C. A. *J. Phys. Chem.* **1982**, *88*, 334–341.

(21) Snyder, R. G.; Strauss, H. L.; Elliger, C. A. *J. Phys. Chem.* **1982**, *86*, 5145–5150.

for the d^+ and d^- modes are consistent with the presence of the surfactants in partially organized micellar microphases. We further simulated the spectral intensities of the methylene and methyl stretching modes using the previously published method²² based on the application of classical electromagnetic theory. Here, the sample structures were modeled as air/surfactant/silicate/Au with equal thicknesses for the surfactant and the silicate phase. In all cases, the exact geometry of the experiment was incorporated in the simulation and the individual layer thicknesses were taken from the ellipsometry data. The optical function spectra for Au and silicate ($1.5 + 0i$) were obtained from the literature²³ while those for the surfactant layer were derived from the transmission FT-IR measurements for the mechanically homogenized pellets consisting of the known concentration bulk surfactant in a KBr matrix.²⁴ The film spectra on Au were simulated for a variety of trial film thicknesses for the surfactant or the silicate layer, and the final thickness was selected on the basis of the best intensity fit of the d^+ and d^- peaks to the experimental spectrum. This procedure yields the overall effective film thickness of ~ 100 nm for the thin film brij56 surfactant-silicate mesophase on Au for films derived at the pulling rate of 20 cm/min. The thicknesses of the films were found to depend strongly on the precise pulling rate, with higher pulling rate yielding thin films of lower thicknesses. A detailed account of these dependences will be separately reported.

Note the presence of a broad envelope spanning 3000–3600 cm^{-1} centered at 3337.4 cm^{-1} for the mesostructured film prior to the ozone treatment. This band is straightforwardly assigned to the hydrogen-bonded silanol groups with adsorbed molecular water at the film's external surface as well as the internal defect sites (due to poor connectivity of the Si–O–Si network in the film interior). In the UV/ozone-treated sample, the maxima of the envelope reveals a large shift and assumes a higher value of 3502.5 cm^{-1} with a distinct sharp band at 3743 cm^{-1} . These shifts clearly indicate that the UV/ozone-treated films display the presence of silanols embedded in noticeably different molecular environments upon template removal. Specifically, the large shift in the envelope peak from the initial 3337.4 to 3502.5 cm^{-1} can be understood in terms of the significant weakening of the H-bonding interactions among the external surface and internal-defect silanol groups. This scenario can be reconciled in terms of the increased silica condensation (as well as subsequent internal defect annihilation) during the UV/ozone treatment (see below), thereby decreasing the number of adjacent geminal and vicinal silanols that participate in H-bonding. Furthermore, the presence of the sharp peak at 3743 cm^{-1} assigned to the free silanol (Si–OH) stretching mode is an unambiguous proof for the appearance of isolated silanol groups upon UV/ozone treatment. We tentatively ascribe this signature almost singularly to the silanols present inside the pore chan-

nels.²⁵ In this regard, we assert that the 3745 cm^{-1} peak can be used as a signature vibrational mode for the pore silanols and can be used to trace/monitor pore chemistries independent of the chemistry occurring at the external surface of the film.

Next, even a casual comparison of the lower frequency regions of the as-formed and UV/ozone-treated samples in Figure 1(b) and (d) reveal the presence of two characteristic modes due to the silicate framework:²⁶ (1) an intense broad band between the 1000 and 1300 cm^{-1} region assigned to the silicate antisymmetric stretching modes, and (2) a broad band in the 900–1000 cm^{-1} region due to silanols. The appearance of the latter band in both precursor and UV/ozone-treated sample spectra confirms the presence of unreacted silanols in both samples and the distinct presence of the former confirms that the inorganic silicate skeleton is preserved during the UV/ozone processing. Furthermore, the intensification of Si–O–Si mode upon the UV/ozone treatment by 55% in integrated intensity suggests that, in addition to removing the organic template, UV/ozone restructures the silicate framework by promoting silanol condensation to form additional Si–O–Si bonds. Similarly, the replacement of the broad silanol peak in the 900–1000 cm^{-1} region with maxima at 937 and 975 cm^{-1} with a single symmetric peak with a maximum at 957 cm^{-1} is consistent with the replacement of unreacted surface and defect silanols in the precursor film by the free silanols in the pore channels upon UV/ozone treatment. Note that the spectra clearly suggest that the UV/ozone treatment did not in any noticeable way disrupt the underlying Au substrate characteristics.

Additional evidence for the silicate restructuring from the initial hexagonal to cubic phase upon UV/ozone exposure is provided by thin film XRD and cross-sectional TEM measurements displayed graphically in Figures 2 and 3, respectively. The XRD data of the as-formed thin film mesophases reveal the presence of three discernible peaks at 1.4028°, 2.84°, and 4.34° with associated d spacings of 62 Å, 31 Å, 20.3 Å, respectively. This is typical of one-dimensional hexagonal (1-dH) mesostructure wherein the three observed peaks can be straightforwardly indexed to be (100), (200), and (300) Bragg planes, leading to the unit cell parameter $a = d_{100} 2/3^{1/2} = 72$ Å. We estimate this periodicity to reflect the center-to-center distance between the hexagonally juxtaposed surfactant-filled channels. The noticeable absence of the peaks due to (110) and (210) reflections in these data further confirm the 1-dH morphology and also suggests that the c -axis of the hexagonal unit cell (or the pore channel) is oriented parallel to the substrate. Additional support for the hexagonal packing is furnished by the TEM images of the scrapped films. By assuming the hexagonal [110] orientation, the observed distance between the parallel bright lines of about 36 Å ($d_{110} = 72/2 = 36$) is entirely consistent with the hexagonal mesostructure. In sharp contrast to the

(22) Parikh, A. N.; Allara, D. L. *J. Chem. Phys.* **1991**, *99*, 927–945.

(23) *Handbook of Optical Constants of Solids II*; Palik, E. D., Ed.; Academic: Orlando, FL, 1985.

(24) The optical tensor contributions of individual vibrational modes were determined by analysis of the transmission spectra of pressed disks of KBr dispersions of polycrystalline samples of the bulk surfactant (see ref 18).

(25) Additional support for this assignment was obtained from a previously published study (Jentys, A.; Kleitorfer, K.; Vinek, H. *Microporous Mesoporous Mater.* **1999**, *27*, 321–328), where it was shown that the topological constraints over the population of silicates in the pores is such as to produce a large number of well-separated isolated silanols that are incapable of participating in H-bonding interactions.

(26) Bellamy, L. J. *The Infrared Spectra of Complex Molecules*; Chapman and Hall: London, 1975; pp 374–383.

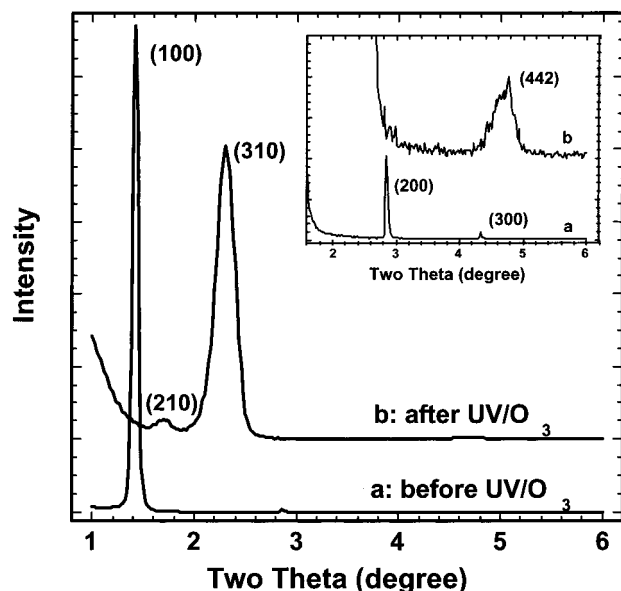


Figure 2. Thin film X-ray diffraction patterns for (a) as-deposited and (b) UV/ozone-treated (solid trace) brij56/TEOS films dip-coated on freshly evaporated Au films.

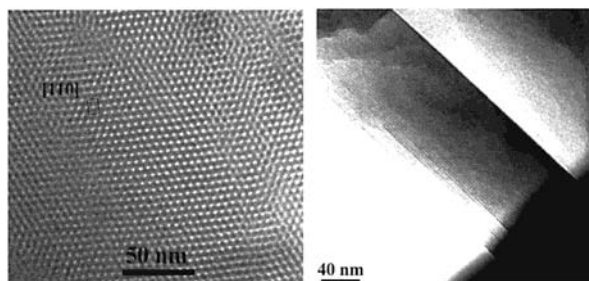


Figure 3. Transmission electron micrograph images for (a) as-deposited and (b) UV/ozone-treated brij56/TEOS films.

above, the XRD traces for the UV/O₃-treated samples reveal a signature typically observed for a complex cubic mesostructure,⁷ confirming the UV/ozone-induced structural transformation of the silicate skeleton upon the template removal. The three peaks observed at 1.71°, 2.3°, and 4.77° can be indexed as (210), (310), and (442) respectively, leading to a primitive cubic unit cell with $a = d_{210} (2^2 + 1^2 + 0^2)^{1/2} = 103 \text{ Å}$. The observed TEM image in Figure 3 (panel b) shows cubic [110] orientation with unit cell $a = 10.3 \text{ nm}$ in direct correspondence with the XRD results.

The thin film porosity was monitored using nitrogen adsorption-desorption isotherm measurements. The data shown in Figure 4 obtained by SAW measurements confirm the formation of pore-channels upon UV/ozone treatment and provide a measure of their structural characteristics consistent with the XRD and TEM data above. The data indicate a type IV isotherms with little or no hysteresis characteristic of mesoporous materials, with the surface area about $310 \text{ m}^2 \text{ g}^{-1}$ and the pore size $\sim 25 \text{ Å}$.

A notable feature of the UV/ozone-based template removal/silicate condensation method is the ability to selectively remove the surfactant microphases from laterally defined regions. The optical micrograph in Figure 5 reveals that the masked areas during UV/ozone treatment reveal different optical contrast than the surface of mesostructured thin film that received the

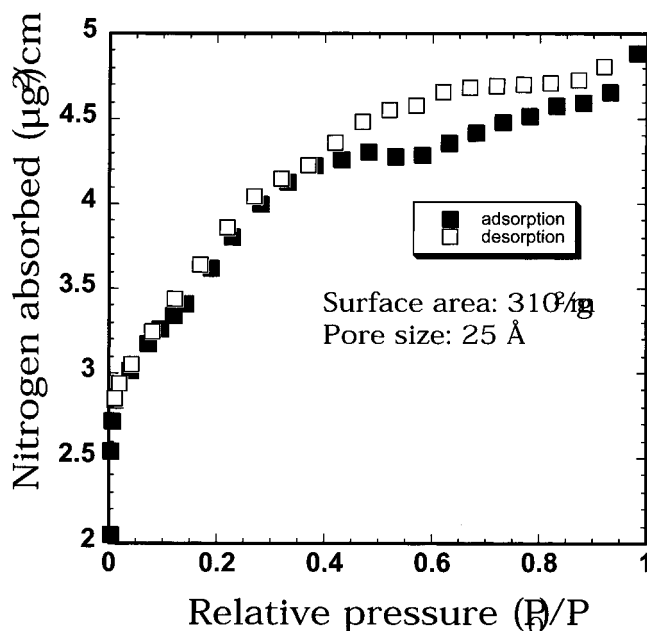


Figure 4. Nitrogen adsorption and desorption isotherm at 77 K for UV/ozone-treated brij56/TEOS films coated on a SAW device.

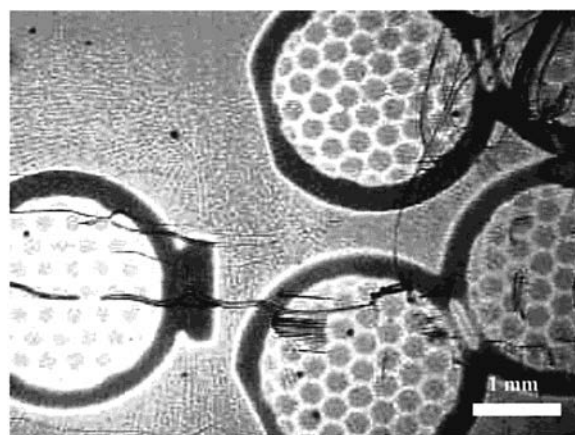


Figure 5. Surface patterns of mesostructured/mesoporous films obtained by the patterned exposure of UV light to a dip-coated Brij56/TEOS film. The brighter region indicate areas that did not receive direct UV exposure. Control experiments suggest that the patterns reflect effective refractive index changes between the exposed and unexposed region due to silicate condensation and surfactant removal.

UV/ozone exposure. We interpret these data to suggest that the template removal and silicate condensation effects of UV/ozone treatment are highly localized.

The ability to pattern mesostructured materials by selective area UV/ozone exposure has an important mechanistic implication. Two independent scenarios can be envisaged. First, it is quite plausible that the ozone produced is rapidly consumed in its reaction with the exposed organic microphase and the inorganic silicate phase. As a result, the diffusion of ozone through the condensed phase of the mesostructured thin film is minimal, allowing for the mask-pattern to be replicated in the final film structure.^{27,28} The second possibility

(27) We believe the observed differences in the color brightness for the UV-unexposed internal grid and the external periphery may be due to differences in the diffusion of ozone through the 56 μm internal grid and $\sim 500 \mu\text{m}$ periphery.

requires that the mechanism of organic phase template removal requires not only ozone oxidation, but also UV exposure. The precise mechanism of UV/ozone-based oxidation of organic material has remained unclear in the literature. For example, Keene and co-workers¹³ suggested that gaseous ozone in the absence of UV light is as effective in the surfactant removal from MCM-41 type solids as UV-generated ozone. In contrast, Moon and co-workers,²⁹ in their UV/ozone study of the removal of organic contaminants from silicon surfaces, showed that ozone alone is ineffective in removing saturated contaminants, but the presence of UV light significantly enhances the process. Our ability to replicate the pattern structure (see Figure 5) is inconclusive in establishing the exact mechanism, but clearly supports that the presence of UV light significantly improves the effect of ozone both in the template removal and in fostering silicate condensation. Additional control experiments will be necessary to establish a complete mechanism. A systematic study is currently being pursued in our laboratory to determine the UV/ozone mechanism of surfactant removal and silicate condensation using a combination of X-ray reflectivity, atomic force microscopy, FT-IR, TEM, and ellipsometric

measurements. These results will be independently reported.

Conclusions

In summary, we showed that the nominally room temperature, UV/ozone treatment provides an efficient means for the removal of surfactant template while simultaneously stabilizing the inorganic silica skeleton into well-defined mesoscopic morphology for a routine production of mesoporous films at low temperatures. The central benefit of the method developed here is the nonthermal processing of the mesostructured precursors. The process is gentle to a wide variety of substrates including thin evaporated metal films, piezoelectric device surfaces, and thin optical waveguide surfaces which, when subjected to the conventional thermal process, undergo considerable pitting, roughening, and occasionally the loss of substrate functionality. Next, the process can be carried out with masks to form patterns and function uniformly for a wide range of substrate geometries. In addition to removing the organic template efficiently, the process fosters the condensation of silica comparable to that offered by the thermal process, and renders the film surfaces highly hydrophilic and the pores water-filled.

Acknowledgment. This work was supported by the Department of Energy and the LDRD program at Los Alamos National Laboratory. T.C. acknowledges partial financial support from the UC President's Postdoctoral Program. Authors acknowledge useful discussions with Dr. A. Shreve.

CM000456F

(28) In a control experiment, we prepared a thin sol-gel film (devoid of the surfactant phase) on an oxidized silicon substrate and exposed it to UV/ozone environment through the pattern-mask. The optical micrographs (not shown) revealed a relief structure of the mask pattern confirming that the localized silicate condensation, in addition to the template phase removal, contributes to the observed pattern. The control experiment further confirms that the effect of ozone is highly localized, presumably due to its rapid reaction with the silicate and the organic microphase in the exposed regions.

(29) Moon, D. W.; Kurokawa, A.; Ichimura, S.; Lee, H. W.; Jeon, I. C. *J. Vac. Sci. Technol. A* **1999**, *17*, 150-154.